IEEE Access
Multidisciplinary | Rapid Review | Open Access Journal

Received April 8, 2018, accepted May 3, 2018, date of publication May 10, 2018, date of current version June 5, 2018.

Digital Object Identifier 10.1109/ACCESS.2018.2834960

Large Scale Remote Sensing Image Segmentation Based on Fuzzy Region Competition and Gaussian Mixture Model

SHOULIN YIN, YE ZHANG, (Member, IEEE), AND SHAHID KARIM
School of Electronics and Information Engineering, Harbin Institute of Technology, Harbin 150000, China

Corresponding author: Ye Zhang (zhye@hit.edu.cn)

This work was supported by the Defense Industrial Technology Development Program under Grant JCKY2016603C004.

ABSTRACT With the ever-increasing amount and complexity of remote sensing image data, the development of large-scale image segmentation analysis algorithms has not kept pace with the need for methods that improve the final accuracy of object recognition. In particular, the development of such methods for large-scale images poses a considerable challenge. Traditional image segmentation methods are of high time complexity and low segmentation accuracy. This paper presents a new large-scale remote sensing image segmentation method that combines fuzzy region competition and the Gaussian mixture model. The new algorithm defines a non-similarity measurement for the class attribute of pixels using the Gaussian mixture model. This algorithm has the ability to perform high precision fitting of data with a statistical distribution, thereby effectively eliminating the influence of noise on the segmentation result. Moreover, fuzzy region competition is introduced to define the prior probability of the neighborhood that will be regarded as the weight of the Gaussian component. This process enhances the robustness of large-scale image segmentation. Finally, we acquire the image data from Google Earth and conduct experiments; the experimental results show that this new method has the feasibility and effectiveness and can achieve highly accurate segmentation results compared with current state-of-the-art methods.

INDEX TERMS Remote sensing image, fuzzy region competition, Gaussian mixture model, large-scale image segmentation.

I. INTRODUCTION

Recently, under the deployment of large-scale sensor networks, a variety of terminal devices are distributed on the various infrastructures to collect information, then the information is sent to the cloud through networks with computing [1]–[4]. After the above process, it is used for support services in different areas. Through information sensing, detection, identification, location, tracking and monitoring, human beings can control the physical world. According to this objective, we study the image segmentation for detect target in real world under cyber computing [5]–[8]. Recent research progress in image segmentation has involved the leveraging of a wide variety of applications in remote sensing, including object detection and image classification [9], [10]. Image segmentation is used for partitioning a remote sensing image into many regions with homogeneous properties that faithfully correspond to the objects [11]. The characteristics of the pixels in the same region are similar, and the characteristics of pixels in different regions are different. Image segmentation is notorious for playing a particularly important role in image processing and computer vision. Remote sensing images contain a large amount of information; however, it is difficult to classify the detail information accurately in images [12]. Therefore, the remote sensing image segmentation issue, especially segmentation for target detection, has attracted considerable attention from many scholars.

To effectively improve the segmentation effect in remote sensing images, many approaches for segmentation have been proposed. Tuia *et al.* [13] proposed a method inspired in the cluster assumption that holds in most of the remote sensing data. Starting from a complete hierarchical description of the data, the proposed strategy aimed at sampling and labeling pixels in order to discover the data partitioning that best matched with the user's expected classes. Therefore, the method combines active supervised and

unsupervised clustering with a smart prune-and-label strategy. Yuan *et al.* [14] utilized both spectral and texture information for remote sensing image segmentation. Linear filters were used to provide enhanced spatial patterns. For each pixel location, they computed combined spectral and texture features using local spectral histograms that concatenated local histograms of all input bands and regarded each feature as a linear combination of several representative features, each of which corresponds to a segment. Yi *et al.* [15] presented a simple scale-synthesis method that was highly flexible, allowing it to be adjusted to meet the segmentation requirements of a variety of image-analysis tasks. This method involves first dividing the whole image area into multiple regions, with each region consisting of ground objects of similar optimal segmentation scale. Next, the suboptimal segmentations of each region are synthesized to obtain the final segmentation result. However, the method was found to be not suited for complex scale images. Mylonas *et al.* [16] proposed an object-based classification scheme for handling remotely sensed images. The method combined the results of a supervised pixel-based classifier with the spatial information extracted from image segmentation. First, pixel-wise classification was implemented by a fuzzy output SVM classifier using the spectral and textural features of pixels. This classification resulted in a set of fuzzy membership maps. Operating on this transformed space, a Genetic Sequential Image Segmentation algorithm was next developed to partition the image into homogeneous regions. Mahesh *et al.* [17] evaluated the effectiveness of a new kernel-based extreme learning machine algorithm for a land cover classification using both multi- and hyperspectral remote-sensing data. The results were compared with the most widely used algorithms-support vector machines and were found to show a good effect.

The image segmentation process is often based on hybrid models for image data modeling. This method divides the image pixels into multiple categories, with each category being known as a data combination of a certain probability distribution in hybrid model. For example, with the most commonly used Gaussian mixture model, each class has its own data mean and variance. Moreover, in further image segmentation, the mean and variance of each class will be considered to be indispensable parameters in the process of segmentation. The resulting parameter combination is optimized by a certain method, thereby completing the classification of all pixels in the image, i.e., the image segmentation is completed.

II. RELATED WORKS

Numerous elaborate methods based on partial differential equations (PDEs) are used widely in the image segmentation field. The active contour model based on variational method and horizontal set method reflects the superiority of PDE segmentation [18]. Shafiq *et al.* [19] proposed an edge-based active contour with an arc length penalty using level set implementation for interpreter-assisted salt dome segmentation. An edge function was designed to study the effect of varying different active contour parameters on salt dome boundary detection. Segmentation methods based on edge information are easy to converge in the edge for which the Grey value changes significantly. However, in fuzzy boundaries or a gradient area, segmentation methods will lead to evolution shaking or crossing of the border. In addition, the image noise can cause interference when attempting to precisely extract an image contour. Although it is possible to first filter an image, because of the weakened edge information, the filtered image is more difficult to subsequently process. To address this issue, an automatic selection of localized region-based active contour model based on image content and its application on brain tumor segmentation was presented [20]. Abdelsamea *et al.* [21] proposed a new supervised active contour model named the Self-Organizing Active Contour (SOAC) model, which combined a variational level set method with the weights of the neurons of two Self-Organizing Maps (SOMs) to process images containing regions characterized by intensity inhomogeneity. The primary contribution of the SOAC model was the development of a new active contour models energy functional optimized in such a manner that the topological structure of the underlying image intensity distribution was preserved-using the two SOMs- in a parallel-processing and local manner. The model is solved by a fast dual projection algorithm under the framework of the classical C-V (region segmentation) model, and the solution speed for global minimum value of the energy function is accelerated.

Based on the regional segmentation model, this model utilizes the continuity of the image as the curve evolution stop criterion to overcome the shortcoming of the poor segmentation effect of the image with poor contrast ratio. Simultaneously, excessive segmentation is often produced, such as dividing the image into many regions; such excessive segmentation cannot achieve the purpose and effect of image analysis. Furthermore, in the process of decision-making, the model does not contain the boundary constraints in regional framework, and segmentation results may appear noise boundary or empty. Therefore, segmentation methods involving synthesizing boundary and area information gradually has become a popular research topic [22]–[24]. For example, the fuzzy region competition algorithm based on region competition uses the fuzzy membership degree to reflect that a pixel may belong to multiple classes. The advantage of this algorithm is that it does not depend on the initialization problem, thus changing the energy function optimization problem into finding the global optimal problem at the convex set. We also notice that most of the existing algorithms adopt simple statistical information in the spatial domain, but the actual image features are relatively complicated. The simple statistical information is not adequate to completely express the images' region information. For example, Choy *et al.* [25] presented a multiphase fuzzy region competition model that took into account spatial and frequency information for image segmentation. In the proposed

energy functional, each region was represented by a fuzzy membership function and a data fidelity term that measured the conformity of spatial and frequency data within each region to Gaussian densities, whose parameters were determined jointly with the segmentation process. Li *et al.* [26] proposed a multiphase fuzzy region competition model for texture image segmentation. In the functional, each region was represented by a fuzzy membership function and a probability density function that is estimated by a non-parametric kernel density estimation.

Generally, cluster methods based on a fuzzy set are effectively used for processing redundant information. To further improve the precision of the fuzzy clustering algorithm, improving the object function and defining the appropriate similarity measure is an effective approach. Because the traditional fuzzy clustering algorithms [27]–[28] use the clustering center on behalf of the class attribute, the non-similarity measure is generally defined as the Euclidean distance between pixels and clustering centers [29]. However, this expression method is not accurate, as it cannot effectively distinguish the distribution of the non-spherical clustering and cannot subdivide the details information. The non-similarity segmentation algorithm of Euclidean measure is sensitive to noise, and the segmentation results are easily affected by the shape density and size of the cluster (i.e., distribution and number of pixel feature in Homogeneous area); moreover, it strongly depends on the initial clustering center and thus cannot be effectively used for large scale remote sensing image segmentation. Consequently, methods based on Gaussian distribution are used for characterizing clustering, with the Gaussian distribution function used as a non-similarity measure [30]–[32]. However, these methods adopt the likelihood estimation method, which can easily fall into a local optimal solution and result in low segmentation accuracy. The single Gaussian distribution cannot accurately fit multi-modal data.

Therefore, it is expected that incorporating a robust parametric model for characterizing the Gaussian component into the energy functional would help to segment complex remote sensing images.

Motivated by the region competition and the recent research studies on Gaussian mixture model analysis, we propose a new large-scale remote-sensing image segmentation method by combining fuzzy region competition and the Gaussian mixture model. The new algorithm defines the non-similarity measurement for the class attribute of pixels by using the Gaussian mixture model. In the energy functional, the fuzzy membership functions are also introduced to measure the association degree of each pixel to all regions. The new algorithm has the ability of high precision fitting of statistical distribution data. With this advantage, the proposed algorithm can effectively eliminate the influence of noise on the segmentation result. Moreover, the fuzzy region competition is introduced to define the prior probability of the neighborhood that will be regarded as the weight of the Gaussian component. This process enhances the robustness of large-scale image segmentation. Justified by the experiments on different types of remote sensing images, the results reveal that our approach is very competitive to current state-of-the-art segmentation methods.

The remainder of this paper is organized as follows. Section II presents the related works for image segmentation over the past several years. In Section III, fuzzy region competition is assessed briefly. The contributions of fuzzy region competition with the Gaussian mixture model are elaborated in Section IV. Section V reports the experiments and performance evaluation. The study's conclusions are presented in Section VI.

III. FUZZY REGION COMPETITION

Before introducing the fuzzy region competition segmentation method, two related segmentation models should be reviewed first, namely, the Mumford-Shah Model and the Chan-Vese Model. Assume that the image segmentation problem can be explained as follows. Consider a gray-scale image $I : \Omega \to R$, where Ω is the image domain, which is a bounded open subset of R^2. As we all know, the aim of image segmentation is to partition Ω by a certain suitable measure into N regions $(\Omega_i)_{i=1,2,\cdots,N}$, where $j \neq i$, $\Omega_i \cap \Omega_j = \phi$ and $\Omega = \Omega_1 \cup \cdots \cup \Omega_N \cup \Psi$, and $\Psi = \bigcup_{i=1}^{N} \Omega_i$ is the union of boundaries of all regions, by certain suitable measure.

A. MUMFORD-SHAH MODEL

Szallasi *et al.* [33] proposed solving the segmentation problem by minimizing the following energy functional:

$$E_{MS}(f, \Psi) = \mu \int_{\Omega} (I - f)^2 dx + \int_{\Omega \setminus \Psi} |\nabla f|^2 dx + \nu |\Psi| \quad (1)$$

where ∇ is a gradient operator, f denotes a piecewise smooth approximate function of I, Ψ is the union of boundaries of image regions, $|\Psi|$ expresses the total length of the arcs making up the curve, and $\mu > 0$ and $\nu > 0$ are fixed parameters. The first term of (1) requires that f approximates I; the second term indicates that f does not vary significantly on each region Ω_i; the third term requires that the boundaries should be as short as possible.

B. CHAN-VESE MODEL

The piecewise constant Mumford–Shah model based on the level set method was represented Chan and colleagues. Chan and Vese [34] proposed the following minimization method for two-phase segmentation:

$$E_{CV}(\Psi, c_1, c_2) = \mu |\Psi| + \lambda_1 \int_{inside(\Psi)} |I - c_1|^2 \, dx + \lambda_2 \int_{outside(\Psi)} |I - c_2|^2 \, dx \quad (2)$$

where c_1 and c_2 are the average values of inside and outside the curve Ψ, respectively; $\nu > 0$, and $\lambda_1, \lambda_2 > 0$ are weights for the regularizing term and the fitting term, respectively.

In the level set method [35], [36], $\Psi \subset \Omega$ is represented by the zero level set of a Lipschitz function $\phi : \Omega \to R$, such that

$$\begin{cases} \Psi = \{x \in \Omega : \phi(x) = 0\}, \\ inside(\Psi) = \{x \in \Omega : \phi(x) > 0\}, \\ outside(\Psi) = \{x \in \Omega : \phi(x) < 0\}. \end{cases} \tag{3}$$

Thus the level set formulation of the Chan–Vese model is:

$$\begin{aligned} E_{CV}(\phi, c_1, c_2) = \mu \int_\Omega |\nabla H(\phi))|dx \\ + \lambda_1 \int_\Omega |I - c_1|^2 H(\phi)dx \\ + \lambda_2 \int_\Omega |I - c_2|^2 (1 - H(\phi))dx \end{aligned} \tag{4}$$

where $H(\phi)$ is the Heaviside function: $H(\phi) = 1$ if $\phi \geq 0$ and $H(\phi) = 0$ otherwise. The evolution equation of ϕ is:

$$\frac{\partial \phi}{\partial t} = \delta_\varepsilon(\phi)(\mu div(\frac{\nabla \phi}{|\nabla \phi|}) - \lambda_1(I - c_1)^2 + \lambda_2(I - c_2)^2) \tag{5}$$

where $\delta_\varepsilon(\phi)$ is an approximation of the Dirac function $\delta(\phi)$, and c_1 and c_2 are updated by the following formulas:

$$c_1 = \frac{\int_\Omega IH(\phi)dx}{\int_\Omega H(\phi)dx} \tag{6}$$

$$c_2 = \frac{\int_\Omega I(1 - H(\phi))dx}{\int_\Omega (1 - H(\phi))dx} \tag{7}$$

The Chan–Vese model is extended to the multiphase model that can perform 2^n-phase segmentation using n level set functions. The corresponding formula is quite complicated and is omitted here. The Chan-Vese model is essentially a variant of the Mumford-Shah model for which f is chosen to be a piecewise constant function. Observe that the minimizing process seeks the best partition of I by taking only two values, namely, c_1 and c_2, and with one edge Ψ. The Chan-Vese model was then further extended to vector-valued and multiphase cases with promising segmentation results.

C. FUZZY REGION COMPETITION

Fuzzy methods have been applied to edge detection, image segmentation and other aspects of image processing. In the use of fuzzy classifier for image segmentation, competition is added in the selection and refining process. The fuzzy method has the advantage of being a simple model that enables easy calculation of the fuzzy classifier and obtains refined segmentation results via to the competitive process.

Song and Yuille [37] proposed minimizing the following energy:

$$F(\Psi, \{\alpha_i\}) = \sum_{i=1}^{N} \{\frac{\mu}{2} \int_{\partial\Omega_i} ds - \int_{\Omega_i} \log P_i(I|\alpha_i)dx\} \tag{8}$$

where α_i is the parameter in the probability density function P_i. The first term within the braces is the length of the boundary curve $\partial\Omega_i$ for region Ω_i. $\Psi = \cup_{i=1}^{N} \partial\Omega_i$ represents the segmentation boundaries of the entire image. The second term is the sum of the cost for coding the intensity I into region Ω_i by the conditional probability distributions $\log P_i(I|\alpha_i)$.

A general two-phase region competition problem is to minimize the following:

$$\begin{aligned} F(\Psi, \alpha_1, \alpha_2) = \int_{\partial\Omega_1} Qds + \lambda \int_{\Omega_1} r_1(I, \alpha_1)dx \\ + \lambda \int_{\Omega_2} r_2(I, \alpha_2)dx \end{aligned} \tag{9}$$

where Ω is partitioned into Ω_1 and Ω_2, α_i is the region parameter for Ω_i, Q is a positive boundary potential, r_i is the error function for Ω_i, and $\lambda > 0$ is a constant. Instead of directly solving (9) to obtain a hard segmentation of Ω, Mory and Ardon [38] proposed using a fuzzy membership function $u \in BV_{[0,1]}(\Omega)$, which is a space of functions of bounded variations taking their values in [0, 1], to represent the region and minimizing the following two-phase fuzzy region competition energy functional.

$$\begin{aligned} F(\mu, \alpha_1, 1\alpha_2) = \int_\Omega |\nabla u|dx + \lambda \int_\Omega r_1(I, \alpha_1)udx \\ + \lambda \int_\Omega r_2(I, \alpha_2)(1-u)dx \end{aligned} \tag{10}$$

The fast dual projection method proposed by Chambolle [39] is used to solve the problem.

IV. PROPOSED SEGMENTATION METHOD

In this section, we will introduce details of the proposed segmentation method, which effectively utilizes the Gaussian mixture model and fuzzy region competition.

A. FUZZY SEGMENTATION MODEL

Let $X = \{x_1, x_2, \cdots, x_n\}$ denote the large-scale remote sensing image, where j is the pixel index and n is the image pixel number. Fuzzy membership function u_{ij} is used for describing the subordination of cluster i to pixel j. Set $U = [u_{ij}]_{c \times n}$ as the fuzzy membership matrix to represent the fuzzy segmentation of image X. c is the homogeneous region number in the pre-segmentation. To determine the optimal U, the non-similarity measure between pixel and cluster must be defined. Next, an objective function is measured. Additionally, it minimizes the objective function to obtain the optimal fuzzy segmentation result. In the fuzzy region competition exponential weighting is used to denote the fuzzy degree, which lacks clear physical meaning. Therefore, the KL regularization item [40] is added into the arithmetic weight to define the objection function.

$$J \triangleq \sum_{j=1}^{n} \sum_{i=1}^{c} u_{ij} d_{ij} + \lambda \sum_{j=1}^{n} \sum_{i=1}^{c} u_{ij} \ln(\frac{u_{ij}}{w_{ij}}) \tag{11}$$

where d_{ij} is the non-similarity measure between pixel and cluster. w_{ij} denotes the prior probability of pixel j belonging to cluster i. The right side of the equation (11) is the KL regularization item, which is conducive to smooth the

change and enhance the segmentation accuracy. $1 < \lambda < \infty$ is the fuzzy factor used for controlling the fuzzy degree. When $\lambda \to 1$, each $u_{ij} \to 0$. Thus, each pixel belongs to the cluster more obviously. If $\lambda = 1$, then the fuzzy cluster method is implemented as a specific algorithm. If $\lambda \to +\infty$, $u_{ij} \to 1/c$.

The Gaussian mixture model is adopted to define the non-similarity measure of image statistical distribution as:

$$P(x_j|w_j, v, \Re) = \sum_{i=1}^{c} w_{ij} p(x_j|v_i, \Re_i) \tag{12}$$

$$p(x_j|v_i, \Re_i) = \frac{1}{(2\pi)^{q/2}|\Re_i|^{1/2}} e^{-1/2(x_j - v_i)\Re_i^{-1}(x_j - v_i)} \tag{13}$$

where $w_j = \{\omega_{ij}; i = 1, 2, \ldots, c\}$ is the prior probability vector. The clustering mean vector set is $v = \{v_i\}$. $\Re = \{\Re_i\}$ is the set of covariance matrices. v_i and $\Re_i$ are the mean vector and covariance matrix, respectively. The non-similarity measure can be defined as the negative logarithmic of the j-th component:

$$\begin{aligned} d_{ij} &\triangleq -\ln w_{ij} p(x_j|v_i, \Re_i) \\ &= \frac{q}{2}\ln(2\pi) + \frac{1}{2}\ln[|\Re_i|] \\ &\quad + \frac{1}{2}((x_j - v_i)^T \Re_i^{-1}(x_j - v_i)) - \ln w_{ij} \end{aligned} \tag{14}$$

For a special region Ω_i in an image, the gray value is distributed independently. The value's corresponding probability distribution can be denoted as $P_i(I|\alpha_i)$ and α_i is the corresponding parameter of P_i. Thus, the energy function of the object and background segmentation is:

$$\begin{aligned} E(\alpha_1, \alpha_2, u) = \int_\Omega |\nabla u| dx + \lambda \Big(\int_\Omega (-u \log P_1(W_A|\alpha_1) \\ - (1-u) lohP_2(W_A|\alpha_2)) dx \end{aligned} \tag{15}$$

P_i must be refined. Under the estimating region parameter, there

$$\begin{aligned} P_i(W_A|\alpha_i) &= P_i(\mu, \sigma_i^2) \\ &= \frac{1}{\sigma_i\sqrt{2\pi}} e^{-\frac{(W_{A(y)}^S - \mu_i)^2}{2\sigma_i^2}} \end{aligned} \tag{16}$$

B. SOLVING THE SEGMENTATION MODEL

Given U and V as well as the solving region parameter $\alpha_i = (\mu_i, \sigma_i^2)$, the energy function can be expressed as

$$\min_\alpha \{E_u(\alpha) = \lambda \int_\Omega u r(W_A, \alpha_1, \alpha_2) dx\} \tag{17}$$

Supposing the given region parameter α and the solving fuzzy membership function u, the energy function can be expressed as

$$\min_{0 \le u \le 1} \{E_\alpha(u) = \int_\Omega |\nabla u| dx + \lambda \int_\Omega u r(W_A, \alpha_1, \alpha_2) dx \tag{18}$$

We first derive the partial differential equation of μ_i and σ_i to obtain region estimation $\hat{\alpha}_i = (\hat{\mu}_i, \hat{\sigma}_i^2)$.

Algorithm 1 Proposed Method

1) Set cluster number c, fuzzy factor λ, fuzzy membership function u and v, $u^1 = 1/\max(I)$, $v^0 = u^1$, and the terminal condition ε.

2) Use $w_{ij} \triangleq \frac{\exp[-b \sum_{j' \in N_j} V_c(l_{j'}, l_j)]}{\sum_{k=1}^{c} \exp[-b \sum_{j' \in N_j} V_c(l_{j'}, l_j)]}$ to calculate the prior probability.

3) Use (14) to obtain the non-similarity measure.

4) Use u_{ij} and (19) to update the membership and region parameter respectively.

5) If $||U^{t+1} - U^t|| < \varepsilon$, then this algorithm stops; otherwise, return step 2.

Let $\omega = u_i / \int_\Omega u_i dx$, where $u_1 = u$, $u_2 = 1 - u$. We obtain

$$\begin{cases} \hat{\mu}_i = \int_\Omega \omega_i \bar{W}_A dx \\ \hat{\sigma}_i^2 = \int_\Omega \omega_i (\bar{W}_A)^2 dx - (\int_\Omega \omega_i \bar{W}_A dx)^2 \end{cases} \tag{19}$$

C. FUZZY MEMBERSHIP FUNCTION UPDATING

To accelerate the solution speed of energy function, a fast iteration algorithm is introduced in this part [41]. An auxiliary variable υ is adopted to realize the function regularization and guarantee data fidelity. In particular, we use υ to replace u,

$$\begin{aligned} E(\alpha, u, \upsilon) = \int_\Omega |\nabla u| dx + \lambda \int_\Omega \upsilon r(W_A, \alpha_1, \alpha_2) dx \\ + \frac{\mu}{2} \int_\Omega (u - \upsilon - d)^2 dx \end{aligned} \tag{20}$$

where μ is a positive number. Thus, we obtain the followings:

$$\begin{aligned} \upsilon^n = \arg\min_{0 \le \upsilon \le 1} \{\lambda \int_\Omega \upsilon r(W_A, \alpha_1, \alpha_2) dx \\ + \frac{\mu}{2} \int_\Omega (u - \upsilon - d)^2 dx\} \end{aligned} \tag{21}$$

$$d^n = d^{n-1} + \upsilon^n - u^n \tag{22}$$

$$u^n = \arg\min_u \{\lambda \int_\Omega |\nabla u| dx + \frac{\mu}{2} \int_\Omega (u - \upsilon - d)^2 dx\} \tag{23}$$

We further obtain the following equations:

$$\upsilon^n = u^n - d^{n-1} - \frac{\lambda}{\mu} \cdot r \cdot (W_A, \alpha_1, \alpha_2) \tag{24}$$

$$\upsilon^n = \max(\min(\upsilon^n, 1), 0) \tag{25}$$

$$\begin{cases} b_x^n = \nabla_x u^n + b_x^{n-1} \\ b_y^n = \nabla_y u^n + b_y^{n-1} \end{cases} \tag{26}$$

$$u^{n+1} = \upsilon^n + d^n - \frac{a}{\mu}(\nabla_x^T b_x^n + \nabla_y^T b_y^n) \tag{27}$$

Algorithm 1 shows the detailed process of our proposed method.

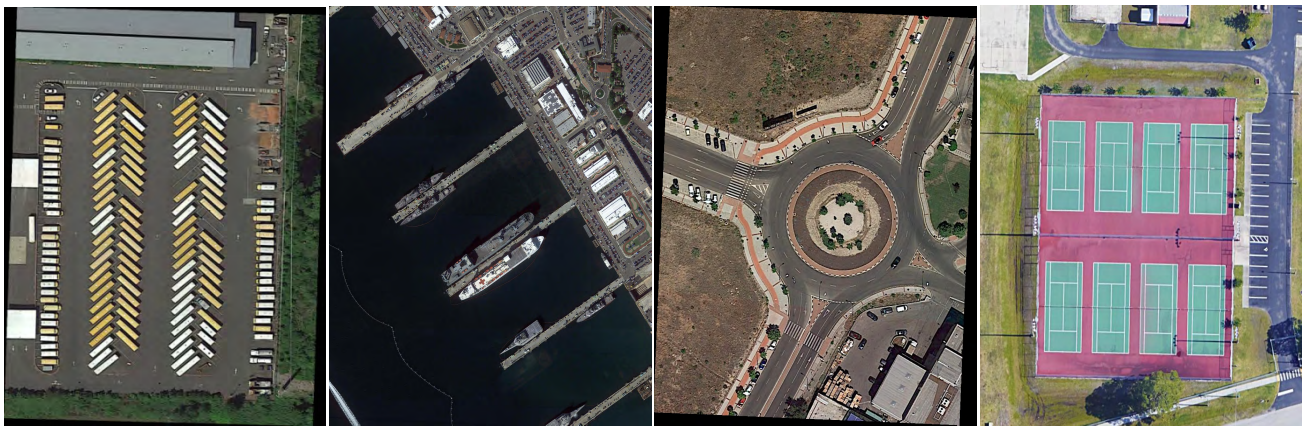

(a) (b) (c) (d)

FIGURE 1. Testing image. (a) large-scale vehicle; (b) ship; (c) roundabout; (d) Tennis court.

V. EXPERIMENTS AND ANALYSIS

To verify the superiority of the proposed large-scale remote sensing image segmentation method (FRCGMM) via combination of fuzzy region competition and the Gaussian mixture model, we perform experiments on remote sensing images obtained from Google earth; the experiments are implemented on a Lenovo computer, RAM 8GB, Intel(R) Core i7-3632QM, CPU 2.2GHz running a Windows 8.1 environment and MATLAB R2017a. We set c, λ and ε as 5, 0.6 and 0.1 respectively, based on the results of exhaustive experiments. The data contains 2806 aerial images from different sensors and platforms and 15 common object categories in these images. We performed many experiments on these objects in the laboratory. In this paper, we only show the test results of four images. Figure 1(a∼d) are the testing images with four object categories (large-vehicle, ship, roundabout and tennis court) considered. The size of each image is 4000×4000 pixels.

A. EVALUATION INDEX

Image segmentation results are quantitatively evaluated by a common measure, i.e., misclassification error (ME) [42]. ME regards image segmentation as a pixel classification process. It measures the percentage of background pixels that are incorrectly classified into foreground (object) pixels, and conversely, the percentage of object pixels erroneously classified into background pixels. For a two class segmentation issue, ME is defined as,

$$ME = 1 - \frac{|bac_1 \cap bac_2| + |for_1 \cap for_2|}{|bac_1| + |for_1|} \tag{28}$$

where bac_1 and for_1 denote the background and foreground of the ground truth (manual segmentation result), respectively, bac_2 and for_2 denote the background and foreground of an image segmentation result, respectively, and $|\cdot|$ denotes the cardinality of a set. The value of ME varies between 0 for a perfectly classified image to 1 for a totally erroneously classified one. A lower value corresponds to better segmentation accuracy

The other evolution index is RSA (region-based segmentation accuracy) [43]. RSA is denoted as

$$P(R; A) = \frac{|R \cap A|}{|R| + |A| - |R \cap A|} \tag{29}$$

Here, $P(R; A)$ is the segmentation accuracy, i.e. the proportion of accurate pixels in the current target block for the ideal target area. R and A are the current segment region and the target region, respectively.

Separation index (S), which uses a minimum-distance separation for partition validity, is given bellow:

$$S = \frac{\sum_{i=1}^{c} \sum_{k=1}^{n} (u_{ik})^2 ||x_k - u_i||^2}{n \min\limits_{1 \le i \le c, 1 \le k \le n} ||x_j - u_i||^2} \tag{30}$$

Another important factor on effectiveness is running time. We will present the detailed data in the next section.

B. COMPARISON EXPERIMENTS FOR LARGE-SCALE IMAGES

We compare FRCGMM with the state-of-the-art methods for large-scale image segmentation of SLSFRC [44] and HBFC [45]. The SLSFRC is a set with selective local and global segmentation; it selectively penalizes the level set function to be binary, and then implements regularization by using Gaussian smoothing. This approach can effectively eliminate the effect of noise. HBFC determines the initial cluster centers and generates a population of initial clustering solutions and then uses an evolutionary algorithm to search for better clustering solutions; at each iteration, the fuzzy c-means method is applied on each initial clustering solution to produce its segmentation result.

First to display a better visual perception, the edge detection results are shown in figure2 with three popular methods of TRM [46], GCA [47], and MDPC [48], as well as our enhanced fuzzy region competition (EFRC) for each image.

And the segmentation results are obtained as shown in figure3. From the results of the first image large-scale vehicle, we can see that the segmentation image obtained by

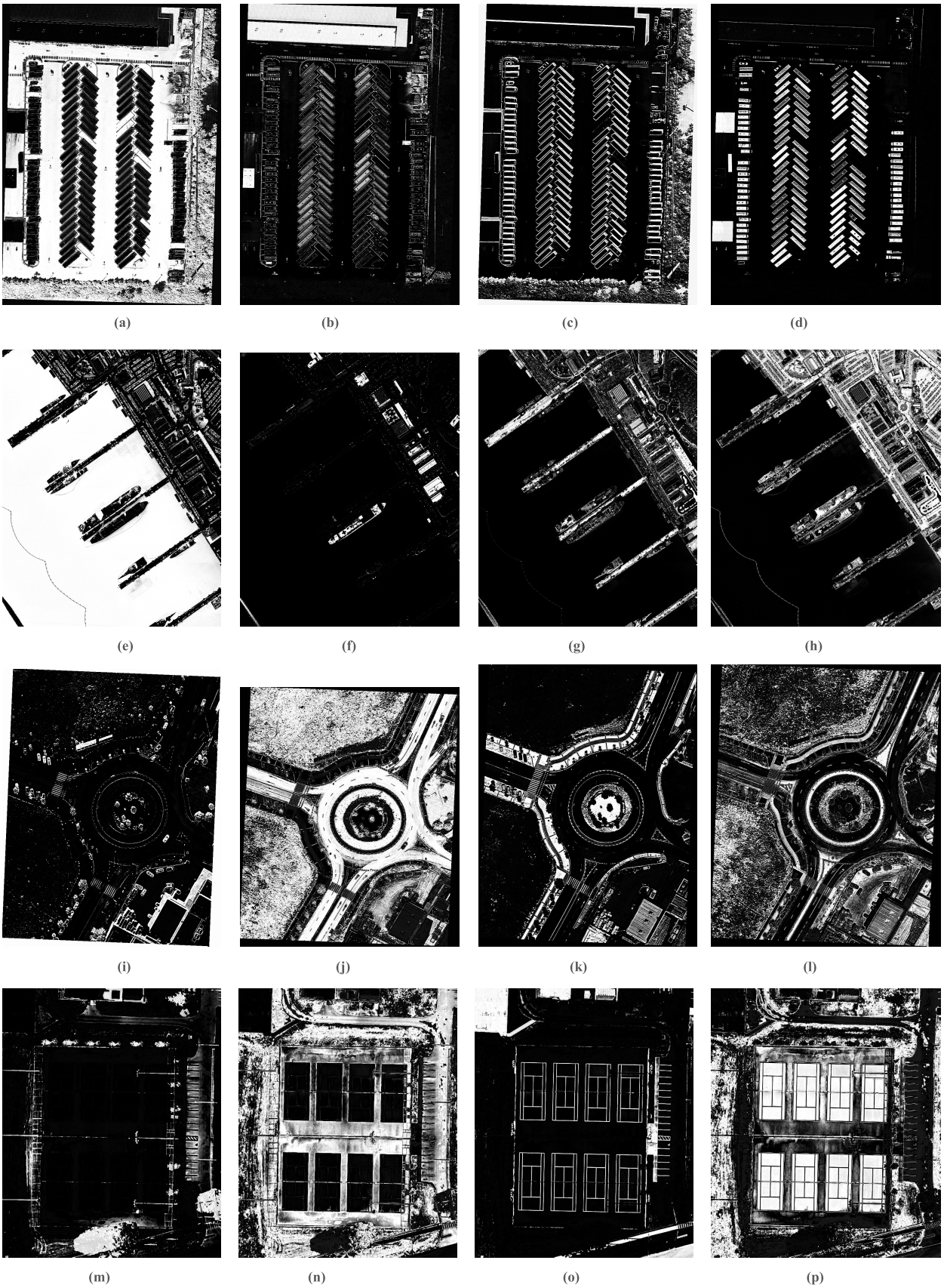

FIGURE 2. Edge detection result. (a-d) TRM method, GCA method, MDPC, EFRCfor large-vehicle; (e-h) For ship; (i-l) For roundabout; (m-p) For tennis court.

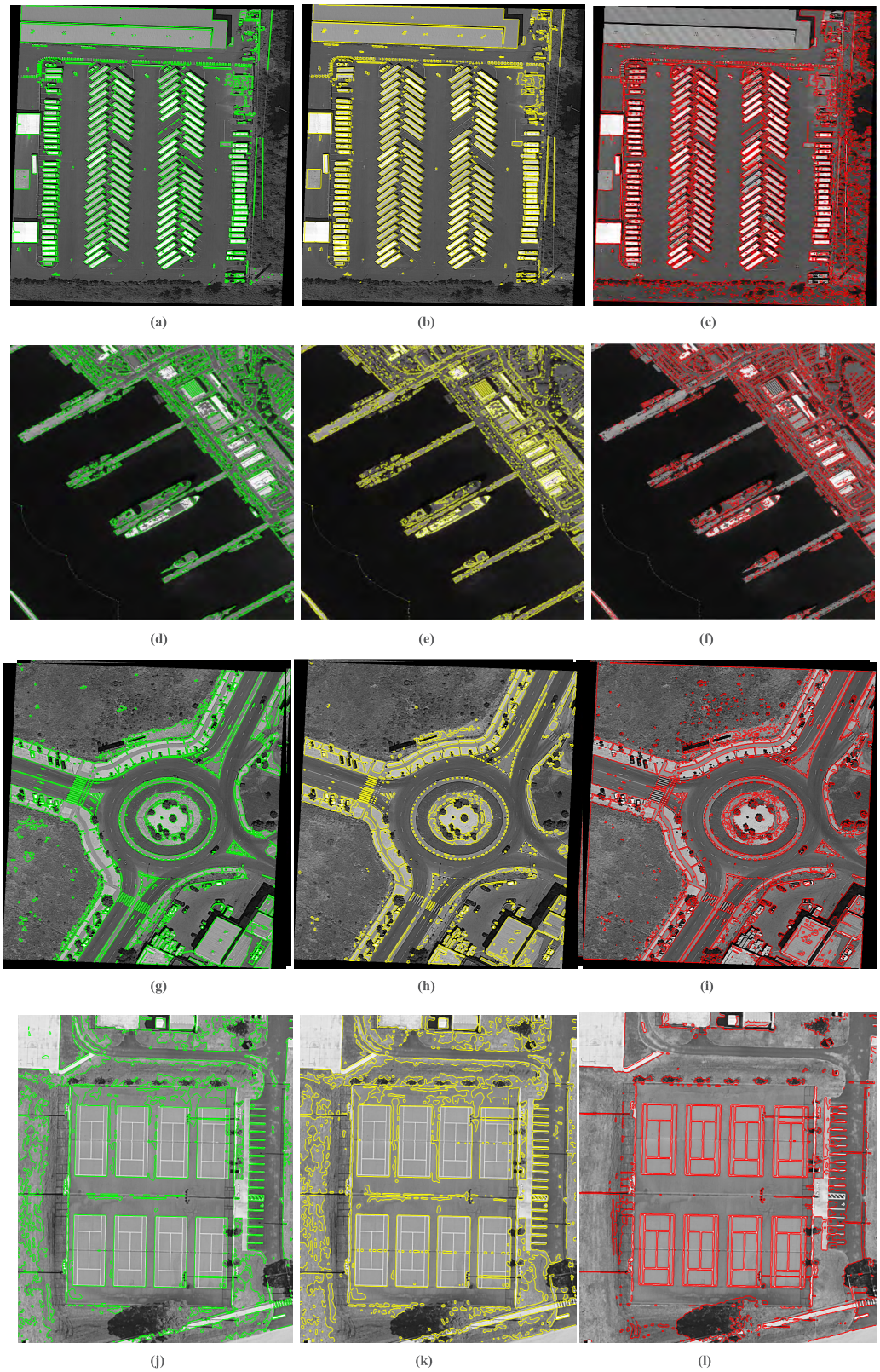

FIGURE 3. Image segmentation. From top to bottom, the results are for large-vehicle, ship, roundabout and tennis court. (a)(d)(g)(j) segmentation results of SLSFRC; (b)(e)(f)(k) segmentation results of HBFC; (c)(f)(i)(l) segmentation results of FRCGMM.

FRCGMM is better than others because its outline is more clear, especially the quadrangle areas of the vehicles. Moreover, according to Table 1, the values of ME of FRCGMM are slightly better than SLSFRC and HBFC. FRCGMM achieves a better segmentation effect in terms of P(R;A) and S than the other two methods.

TABLE 1. Comparison of the three methods on the large-vehicle image.

Metric	ME	P(R;A)	S
SLSFRC	0.182	87.8%	0.097
HBFC	0.091	89.4%	0.158
FRCGMM	0.067	96.5%	0.416

And the segmentation results are obtained as shown in figure3. From the results of the first image large-scale vehicle, we can see that the segmentation image obtained by FRCGMM is better than others because its outline is more clear, especially the quadrangle areas of the vehicles. Moreover, according to Table 1, the values of ME of FRCGMM are slightly better than SLSFRC and HBFC. FRCGMM achieves a better segmentation effect in terms of P(R;A) and S than the other two methods.

For the second image of a ship, FRCGMM achieves the best ME and S values among all the algorithms; these values are far greater than those of the other algorithms as displayed in table 2, but its value of P(R;A) is close to those of the other methods. Therefore, FRCGMM obtains a good segmentation effect. Generally, the image of FRCGMM may be the best one showing obvious features, i.e., the beach and deck in figure3.

TABLE 2. Comparison of the three methods on the ship image.

Metric	ME	P(R;A)	S
SLSFRC	0.197	94.1%	0.164
HBFC	0.103	93.4%	0.278
FRCGMM	0.052	95.9%	0.532

On the image of the roundabout, FRCGMM shows better performance than other methods, and its images embody clear edges and show significant characteristics. For the outer ring and the bottom right corner, the segmentation effect of HBFC is not obvious enough. Hence, FRCGMM shows preferable segmentation effect on the background clearly and provides more clear edges. The results shown in table 3 demonstrate that the proposed method has better effect than the other methods. The similar result of the tennis court is shown in table 4.

FRCGMM reveals the best overall performance among the three methods, because it combines fuzzy region competition and the Gaussian mixture model to better balance segmentation than the other algorithms and thus achieves segmentation results that better balance the intra-class polymerization and the inter-class difference. Therefore, in most conditions we recommend the use of our proposed segmentation method.

TABLE 3. Comparison of the three methods on the roundabout image.

Metric	ME	P(R;A)	S
SLSFRC	0.188	91.2%	0.087
HBFC	0.132	94.5%	0.193
FRCGMM	0.048	96.7%	0.486

TABLE 4. Comparison of the three methods on the tennis court image.

Metric	ME	P(R;A)	S
SLSFRC	0.192	92.2%	0.113
HBFC	0.143	95.1%	0.172
FRCGMM	0.054	97.2%	0.509

C. COMPARISON OF RUNNING TIME

We provide the run-time of SLSFRC, HBFC and FRCGMM for the large-vehicle, ship, roundabout and tennis court as listed in figure4. Because they use different super-pixel generation methods, we do not contain the computational cost for super-pixel generation. Moreover, the average time cost of the proposed method is better than that of HBFS and SLSFRC, because the Gaussian mixture model accelerates the learning procedure. Fuzzy region competition helps reduce the computational burden of the learning procedure, and thus leads to a more efficient and convenient interactive image segmentation system. The low cost of our proposed method implies that FRCGMM is suitable for large-scale images that have a large number of super-pixels. Overall,

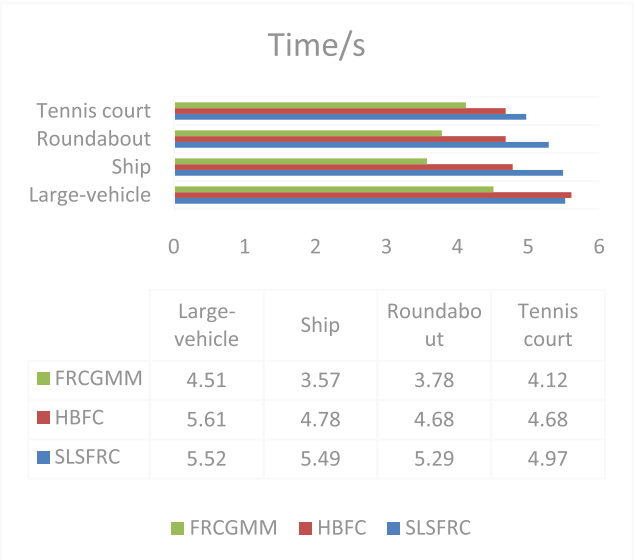

FIGURE 4. Running time (in seconds) on the testing images.

the proposed method achieves satisfactory image segmentation results with very low computational cost.

D. DISCUSSION FOR SMALL SCALE IMAGES

Although we performed segmentation experiments for large-scale remote sensing images, we must explore whether this method is suitable for small-scale images. The experiments are conducted on four single object real world images with size of 400×400. The original images are exhibited in figure 5. To save space, the visual segmentation results obtained by various methods are not listed in this paper. To ensure the fairness of the experiment, we selected another two famous methods for the small scale images of EDCS (Edge Density Contrast Stretching) [49] and SLGS (Selective Local and Global Segmentation) [50] for comparison with our proposed method. The segmentation results are shown in figure 6 for the three images.

FIGURE 5. Original images. (a) pepper; (b) Lena; (c) Baboon.

Quantitative performance comparisons of various methods are listed in table 5, table 6 and table 7. To save space, we use the evaluation index described in section 5.1 to determine the performance. The comparison tables show that the ME value of FRCGMM is dramatically lower than those of other methods, i.e., FRCGMM has the best average segmentation accuracy. In addition, FRCGMM obtains lower S values compared to the other methods, indicating that FRCGMM has better stability.

TABLE 5. Comparison of the three methods on image pepper.

Metric	ME	P(R;A)	S
EDCS	0.209	89.8%	0.351
SLGS	0.233	96.7%	0.228
FRCGMM	0.073	98.5%	0.637

TABLE 6. Comparison of the three methods on image Lena.

Metric	ME	P(R;A)	S
EDCS	0.185	91.8%	0.358
SLGS	0.178	96.9%	0.322
FRCGMM	0.069	98.6%	0.712

We also conducted experiments of computational time for the three methods, as listed in figure 7. For the

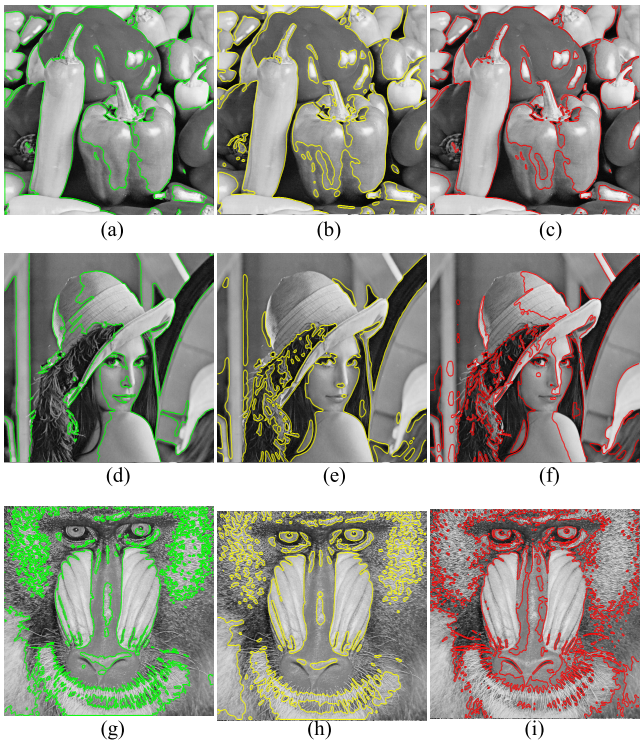

FIGURE 6. Ma Image segmentation results. From top to bottom, the results are for pepper, Lena, Baboon. (a) (d) (g) segmentation results of EDCS; (b)(e)(h) segmentation results of SLGS; (c)(f)(i) segmentation results of proposed method.

TABLE 7. Comparison of the three methods on image baboon.

Metric	ME	P(R;A)	S
EDCS	0.118	89.4%	0.198
SLGS	0.124	92.3%	0.261
FRCGMM	0.057	95.8%	0.569

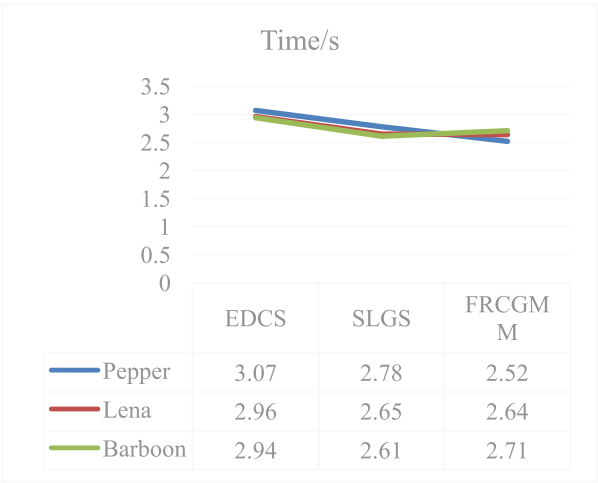

FIGURE 7. Computational time (in seconds) on the testing images.

computational time, the differences are small, indicating that FRCGMM has a similar effect compared to the other methods.

In summary, the proposed FRCGMM effectively segments the testing images and achieves clear results, which shows the combination of fuzzy region competition and the Gaussian mixture model is beneficial to improve the accuracy and precision of image segmentation. A shortcoming of FRCGMM is that its P(R;A) values are typically closely to those of other methods for small-scale images indicating that overlapping between the resultant segmentation is unremarkable. However, the effect is considerably better. Overall, the proposed method achieves satisfactory image segmentation result

VI. CONCLUSION

To overcome the shortcomings of the fuzzy region competition method, a large scale remote sensing image segmentation method combining fuzzy region competition and the Gaussian mixture model was proposed under cyber computing. In the proposed method, non-similarity measurement for the class attribute of pixels is defined using the Gaussian mixture model. This new algorithm is able to achieve high precision fitting of statistical distribution data, thus effectively eliminating the influence of noise on the segmentation result. Moreover, the fuzzy region competition is introduced to define the prior probability of the neighborhood that is regarded as the weight of the Gaussian component. This process was found to greatly enhance the robustness of large scale image segmentation. Through adding the Gaussian mixture model, the whole image can preserve the original data coherence. The experimental results on a series of large-scale remote sensing images and single-object real world images demonstrated that the proposed method significantly improves segmentation accuracy and robustness in comparison with existing transition region-based image thresholding methods, as well as other segmentation techniques. In the future, we will develop more advanced artificial intelligence algorithms to segment images and apply them to real engineering practices.

REFERENCES

[1] Q. Zhang, L. T. Yang, Z. Chen, and P. Li, "A survey on deep learning for big data," *Inf. Fusion*, vol. 42, pp. 146–157, Jul. 2018.

[2] J. Gao, J. Li, and Y. Li, "Approximate event detection over multi-modal sensing data," *J. Combinat. Optim.*, vol. 32, no. 4, pp. 1–15, 2015.

[3] P. Li, Z. Chen, L. T. Yang, Q. Zhang, and M. J. Deen, "Deep convolutional computation model for feature learning on big data in Internet of Things," *IEEE Trans. Ind. Informat.*, vol. 14, no. 2, pp. 790–798, Feb. 2017.

[4] Q. Zhang, L. T. Yang, Z. Chen, P. Li, and F. Bu, "An adaptive droupout deep computation model for industrial IoT big data learning with crowdsourcing to cloud computing," *IEEE Trans. Ind. Informat.*, to be published.

[5] P. Li, Z. Chen, L. T. Yang, L. Zhao, and Q. Zhang, "A privacy-preserving high-order neuro-fuzzy c-means algorithm with cloud computing," *Neurocomputing*, vol. 256, pp. 82–89, Sep. 2017.

[6] Q. Zhang, L. T. Yang, Z. Chen, and P. Li, "An improved deep computation model based on canonical polyadic decomposition," *IEEE Trans. Syst., Man, Cybern., Syst.*, to be published.

[7] J. Gao, J. Li, Z. Cai, and H. Gao, "Composite event coverage in wireless sensor networks with heterogeneous sensors," in *Proc. IEEE Comput. Commun.*, Apr./May 2015, pp. 217–225.

[8] Q. Zhang, Z. Chen, and Y. Leng, "Distributed fuzzy c-means algorithms for big sensor data based on cloud computing," *Int. J. Sensor Netw.*, vol. 18, nos. 1–2, p. 32, 2015.

[9] S. Gupta, P. Arbeláez, R. Girshick, and J. Malik, "Indoor scene understanding with RGB-D images: Bottom-up segmentation, object detection and semantic segmentation," *Int. J. Comput. Vis.*, vol. 112, no. 2, pp. 133–149, 2015.

[10] H. Cholakkal, J. Johnson, and D. Rajan, "A classifier-guided approach for top-down salient object detection," *Signal Process. Image Commun.*, vol. 45, pp. 24–40, Jul. 2016.

[11] L. He *et al.*, "A comparative study of deformable contour methods on medical image segmentation," *Image, Vis. Comput.*, vol. 26, no. 2, pp. 141–163, 2008.

[12] M. Pinheiro and J. L. Alves, "A new level-set-based protocol for accurate bone segmentation from CT imaging," *IEEE Access*, vol. 3, pp. 1894–1906, 2015.

[13] D. Tuia, J. Muñoz-Marí, and G. Camps-Valls, "Remote sensing image segmentation by active queries," *Pattern Recognit.*, vol. 45, no. 6, pp. 2180–2192, 2012.

[14] J. Yuan, D. Wang, and R. Li, "Remote sensing image segmentation by combining spectral and texture features," *IEEE Trans. Geosci. Remote Sens.*, vol. 52, no. 1, pp. 16–24, Jan. 2014.

[15] L. Yi, G. Zhang, and Z. Wu, "A scale-synthesis method for high spatial resolution remote sensing image segmentation," *IEEE Trans. Geosci. Remote Sens.*, vol. 50, no. 10, pp. 4062–4070, Oct. 2012.

[16] S. K. Mylonas, D. G. Stavrakoudis, and J. B. Theocharis, "GeneSIS: A GA-based fuzzy segmentation algorithm for remote sensing images," *Knowl.-Based Syst.*, vol. 54, no. 4, pp. 86–102, 2013.

[17] M. Pal, A. E. Maxwell, and T. A. Warner, "Kernel-based extreme learning machine for remote-sensing image classification," *Remote Sens. Lett.*, vol. 4, no. 9, pp. 853–862, 2013.

[18] Y. Zhao, L. Rada, K. Chen, S. P. Harding, and Y. Zheng, "Automated vessel segmentation using infinite perimeter active contour model with hybrid region information with application to retinal images," *IEEE Trans. Med. Imag.*, vol. 34, no. 9, pp. 1797–1807, Sep. 2015.

[19] M. A. Shafiq, Z. Wang, and G. Alregib, "Seismic interpretation of migrated data using edge-based geodesic active contours," in *Proc. IEEE Signal Inf. Process.*, Dec. 2016, pp. 596–600.

[20] E. Ilunga-Mbuyamba, J. G. Avina-Cervantes, J. Cepeda-Negrete, M. A. Ibarra-Manzano, and C. Chalopin, "Automatic selection of localized region-based active contour models using image content analysis applied to brain tumor segmentation," *Comput. Biol., Med.*, vol. 91, pp. 69–79, Dec. 2017.

[21] M. M. Abdelsamea, G. Gnecco, and M. M. Gaber, "An efficient self-organizing active contour model for image segmentation," *Neurocomputing*, vol. 149, pp. 820–835, Sep. 2015.

[22] J. Duan, Z. Pan, X. Yin, W. Wei, and G. Wang, "Some fast projection methods based on Chan–Vese model for image segmentation," *EURASIP J. Image, Video Process.*, vol. 2014, no. 1, p. 7, 2014.

[23] Y. Li, "Wavelet-based fuzzy multiphase image segmentation method," *Pattern Recognit. Lett.*, vol. 53, pp. 1–8, Feb. 2015.

[24] F. Li, S. Osher, J. Qin, and M. Yan, "A multiphase image segmentation based on fuzzy membership functions and L1-norm fidelity," *J. Sci. Comput.*, vol. 69, no. 1, pp. 82–106, 2016.

[25] S. K. Choy, M. L. Tang, and C. S. Tong, "Image segmentation using fuzzy region competition and spatial/frequency information," *IEEE Trans. Image Process.*, vol. 20, no. 6, pp. 1473–1484, Jun. 2011.

[26] F. Li and M. K. Ng, "Kernel density estimation based multiphase fuzzy region competition method for texture image segmentation," *Commun. Comput. Phys.*, vol. 8, no. 3, pp. 623–641, 2010.

[27] Q. Zhang, L. T. Yang, Z. Chen, P. Li, and M. J. Deen, "Privacy-preserving double-projection deep computation model with crowdsourcing on cloud for big data feature learning," *IEEE Internet Things J.*, to be published.

[28] Q. Zhang, L. T. Yang, Z. Chen, and P. Li, "PPHOPCM: Privacy-preserving high-order possibilistic c-means algorithm for big data clustering with cloud computing," *IEEE Trans. Big Data*, to be published.

[29] F. Zhao, L. Jiao, and H. Liu, "Kernel generalized fuzzy c-means clustering with spatial information for image segmentation," *Digit. Signal Process.*, vol. 23, no. 1, pp. 184–199, 2013.

[30] S. Zhou, J. Wang, M. Zhang, Q. Cai, and Y. Gong, "Correntropy-based level set method for medical image segmentation and bias correction," *Neurocomputing*, vol. 234, pp. 216–229, Apr. 2017.

[31] H. Gongt, Y. Li, G. Liu, W. Wu, and G. Chen, "A level set method for retina image vessel segmentation based on the local cluster value via bias correction," in *Proc. IEEE Int. Congr. Image Signal Process.*, Oct. 2016, pp. 413–417.

[32] X. Xin, L. Wang, C. Pan, and S. Liu, "Adaptive regularization level set evolution for medical image segmentation and bias field correction," in *Proc. IEEE Int. Conf. Image Process.*, Sep. 2015, pp. 1006–1010.
[33] D. Mumford and J. Shah, "Optimal approximations by piecewise smooth functions and associated variational problems," *Commun. Pure Appl. Math.*, vol. 42, no. 5, pp. 577–685, 1989.
[34] T. F. Chan and L. A. Vese, "Active contours without edges," *IEEE Trans. Image Process.*, vol. 10, no. 2, pp. 266–277, Feb. 2001.
[35] F. Li, M. K. Ng, T. Y. Zeng, and C. Shen, "A multiphase image segmentation method based on fuzzy region competition," *SIAM J. Imag. Sci.*, vol. 3, no. 3, pp. 277–299, 2010.
[36] J. A. Sethian, *Level Set Methods: Evolving Interfaces in Computational Geometry, Fluid Mechanics, Computer Vision, and Materials Science*. Cambridge, U.K.: Cambridge Univ. Press, 1996.
[37] S. C. Zhu and A. Yuille, "Region competition: Unifying snakes, region growing, and Bayes/MDL for multiband image segmentation," *IEEE Trans. Pattern Anal. Mach. Intell.*, vol. 18, no. 9, pp. 884–900, Sep. 1996.
[38] B. Mory and R. Ardon, "Fuzzy region competition: A convex twophase segmentation framework," in *Proc. SSVM*, 2007, pp. 214–226.
[39] A. Chambolle, "An algorithm for total variation minimization and applications," in *Proc. Conf. Math. Image Anal.*, 2004, pp. 89–97.
[40] H. Ichihashi, K. Miyagishi, and K. Honda, "Fuzzy c-means clustering with regularization by K-L information," in *Proc. IEEE Int. Conf. Fuzzy Syst.*, vol. 2. Dec. 2001, pp. 924–927.
[41] R. Q. Jia and H. Zhao, "A fast algorithm for the total variation model of image denoising," *Adv. Comput. Math.*, vol. 33, no. 2, pp. 231–241, 2010.
[42] W. A. Yasnoff, J. K. Mui, and J. W. Bacus, "Error measures for scene segmentation," *Pattern Recognit.*, vol. 9, no. 4, pp. 217–231, 1977.
[43] S. Wang, "New benchmark for image segmentation evaluation," *J. Electron. Imag.*, vol. 16, no. 3, p. 033011, 2007.
[44] B. N. Li, J. Qin, R. Wang, M. Wang, and X. Li, "Selective level set segmentation using fuzzy region competition," *IEEE Access*, vol. 4, pp. 4777–4788, 2016.
[45] M. Zhang, W. Jiang, X. Zhou, Y. Xue, and S. Chen, "A hybrid biogeography-based optimization and fuzzy C-means algorithm for image segmentation," *Soft Comput.*, vol. 1, pp. 1–14, Dec. 2017.
[46] A. Drogoul and G. Aubert, "The topological gradient method for semilinear problems and application to edge detection and noise removal," *Inverse Problems, Imag.*, vol. 10, no. 1, pp. 51–86, 2017.
[47] B. Qiao, L. Jin, and Y. Yang, "An adaptive algorithm for grey image edge detection based on grey correlation analysis," in *Proc. Int. Conf. Comput. Intell. Secur.*, Dec. 2017, pp. 470–474.
[48] Y. Yang, K. I. Kou, and C. Zou, "Edge detection methods based on modified differential phase congruency of monogenic signal," *Multidimensional Syst., Signal Process.*, vol. 29, no. 1, pp. 1–21, 2018.
[49] H. Ayad, N. F. Hassan, and S. Mallallah, "A modified segmentation approach for real world images based on edge density associated with image contrast stretching," *Iraqi J. Sci.*, vol. 58, no. 581A, pp. 163–174, 2017.
[50] K. Bikshalu and R. Srikanth, "LSF evolution with selective local and global segmentation for synthetic and real images," in *Proc. Int. Conf. Signal Inf. Process.*, 2017, pp. 1–5.

SHOULIN YIN received the B.S. and M.S. degrees from the Software College, Shenyang Normal University, Shenyang, China, in 2013 and 2015, respectively. He is currently pursuing the Ph.D. degree with the School of Electronic and Information Engineering, Harbin Institute of Technology, Harbin, China.

His research interests include image fusion, target detection, and image recognition.

YE ZHANG received the B.S. degree in communication engineering and the M.S. and Ph.D. degrees in communication and electronic systems from the Harbin Institute of Technology (HIT), Harbin, China, in 1982, 1985, and 1996, respectively.

In 1985, he joined HIT as a Teacher. From 1998 to 1999, he was a Visiting Scholar with The University of Texas at San Antonio, San Antonio, TX, USA. He is currently a Professor and a Doctoral Supervisor in information and communication engineering. He is also the Director of the School of Electronic and Information Engineering, Institute of Image and Information Technology, HIT. His research interests are remote sensing hyperspectral image analysis and processing, image/video compression and transmission, and multisource information collaboration processing and applications.

SHAHID KARIM received the B.S. degree in electronics from the COMSATS Institute of Information Technology, Abbottabad, Pakistan, in 2010, and the M.S. degree in electronics and information engineering from Xi'an Jiaotong University, China, in 2015. He is currently pursuing the Ph.D. degree with the Department of Information and Communication Engineering, School of Electronics and Information Engineering, Harbin Institute of Technology, China. His current research interests include image processing, object detection, and classification toward remote sensing imagery.